*Anal. Chem.* **2008,** *80,* 3498−3501

# Optical Biosensor Based On Hollow Integrated Waveguides

**Víctor J. Cadarso,*,† César Fernández-Sánchez,† Andreu Llobera,† Margarita Darder,‡ and Carlos Domínguez†**

*Institut de Microelectrònica de Barcelona, CNM-IMB, CSIC, Campus UAB 08193 Barcelona, Spain, and Instituto de Ciencia de Materiales de Madrid, CSIC, Cantoblanco, 28049 Madrid, Spain*

**The first absorbance biosensor based on pure silicon hollow integrated waveguides is presented in this work. With the use of horseradish peroxidase (HRP) as a model recognition element, an enzymatic sensor for the measurement of hydrogen peroxide was fabricated, numerically simulated, and experimentally characterized. Waveguides with widths ranging from 50 to 80 $\mu$m, having a depth of 50 $\mu$m and lengths up to 5 mm were easily fabricated by just one photolithographic step. These were further modified by covalent immobilization of HRP using silanization chemistry. Simulation studies of the proposed approach showed a sensor linear behavior up to 300 $\mu$M $H_2O_2$ and a sensitivity of $2.7 \times 10^{-3}$ AU/$\mu$M. Experimental results were in good agreement with the simulated ones. A linear behavior between 10 and 300 $\mu$M $H_2O_2$, a sensitivity of $3 \times 10^{-3}$ AU/$\mu$M, and a signal-to-noise ratio around 20 dB were attained. Also, kinetic studies of the activity of the immobilized enzyme on the silicon waveguide surface gave an apparent Michaelis−Menten constant of 0.44 mM. The simple technology proposed in this work enables the fabrication of cost-effective, easy-to-use, miniaturized biosensor generic platforms, these being envisioned as excellent candidates for the development of lab-on-a-chip systems.**

The development of new integrated optical (IO) transducers for optochemical and biosensor applications can overcome the limitations shown by conventional optical sensors. These transducers can be based on several transduction modes. Fluorescence detection,[1] shifts of the refractive index, such as surface plasmon resonance,[2] interferometry,[3] and waveguide coupling[4] detection schemes, as well as absorbance-based protocols[5] have been reported. Although systems with the ability to discriminate between excitation and emission wavelengths have recently been reported,[6] fluorescence spectroscopy techniques generally require complex experimental setups to develop miniaturized sensors with the ability to discriminate very low analytical signals from the background fluorescence. Sensors based on variations of the refractive index present some problems derived from their poor specificity and the interference caused by any physical or chemical parameters that modify the real part of the refractive index, such as temperature, pressure, or other room conditions.

Optical absorbance sensors usually rely on the interaction of the evanescent field (EF) of the guided light with the analyte[7] or the use of microoptic designs, with an optochemical active membrane replacing a section of the waveguide.[8] The former normally requires long interaction distances or having a large EF propagating outside the waveguide, which make them very dependent on variations of the analyte refractive index. The latter involves light propagation in short sensing regions within the waveguide, which gives rise to limited sensitivities of the final devices. Absorbance sensors generally require labeling of the analyte to be detected so as to be provided with a colorimetric response, as opposed to the interferometry-based systems.[9] Additionally, they have lower sensitivity. Nevertheless, their fabrication and characterization is generally simpler, which make them extremely attractive for low-cost applications.

Silicon-based hollow waveguides[10] are well suited for the development of chemical sensors due to their inherent properties such as low attenuation coefficients, the possibility of integrating optics, electronics, and microfluidics on the same structure, and high interaction efficiency.[11] To date, few devices have been fabricated using these structures, which include a gas sensor for the analysis of carbon monoxide and nitric oxide[12] and an integrated silicon microflow cytometer for cell counting.[13]

* To whom correspondence should be addressed.
† Institut de Microelectrònica de Barcelona, CNM-IMB, CSIC.
‡ Instituto de Ciencia de Materiales de Madrid, CSIC.

(1) Taitt, C. R.; Anderson, G. P.; Ligler, F. S. *Biosens. Bioelectron.* **2005**, *20*, 2470−2487.
(2) Mauriz, E.; Calle, A.; Montoya, A.; Lechuga, L. M. *Talanta* **2006**, *69*, 359−364.
(3) Lambeck, P. V. *Meas. Sci. Technol.* **2006**, *17*, R93−R116.
(4) Dumais, P.; Callender, C. L.; Noad, J. P.; Ledderhof, C. J. *IEEE Photon. Tech. Lett.* **2005**, *17*, 441−443.
(5) Puyol, M.; Salinas, I.; Garcés, I.; Villuendas, F.; Llobera, A.; Dominguez, C.; Alonso, J. *Anal. Chem.* **2002**, *74*, 3354−3361.
(6) Llobera A.; Wilke R.; Buttgenbach S. *Lab Chip* **2004**, *4*, 24−27.
(7) Umemura, T.; Hotta, H.; Abe, T.; Takahashi, Y.; Takiguchi, H.; Uehara, M.; Odake, T.; Tsunoda, K. *Anal. Chem.* **2006**, *78*, 7511−7516.
(8) Garces, I.; Villuendas, F.; Salinas, I.; Alonso, J.; Puyol, M.; Dominguez, C.; Llobera, A. *Sens. Actuators, B* **1999**, *60*, 191−199.
(9) Prieto, F.; Sepulveda, B.; Calle, A.; Llobera, A.; Dominguez, C.; Lechuga, L. M. *Sens. Actuators, B* **2003**, *92*, 151−158.
(10) Bernini, R. *IEEE J. Sel. Top. Quantum Electron.* **2002**, *8*, 106−110.
(11) Yin, D. L.; Barber, J. P.; Hawkins, A. R.; Schmidt, H. *Appl. Phys. Lett.* **2005**, *87*, 211111.
(12) Thompson, B. T.; Inberg, A.; Croitoru, N.; Mizaikoff, B. *Appl. Spectrosc.* **2006**, *60*, 266−271.
(13) Bernini, R.; De Nuccio, E.; Brescia, F.; Minardo, A.; Zeni, L.; Sarro, P. M.; Palumbo, R.; Scarfi, M. R. *Anal. Bioanal. Chem.* **2006**, *386*, 1267−1272.



10.1021/ac702293r CCC: $40.75 
Published on Web 04/05/2008

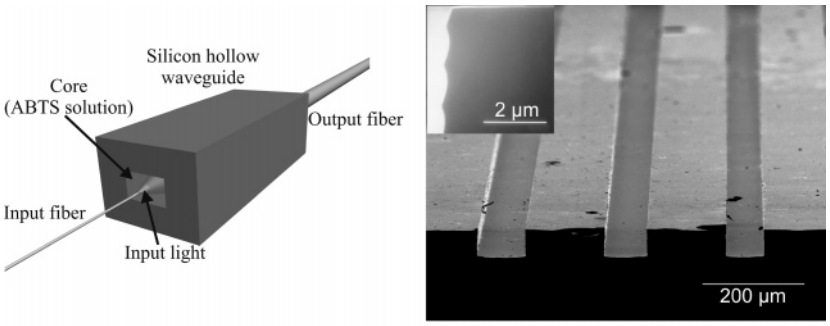


**Figure 1.** (a) Scheme of the optical biosensor setup with the input and output fiber optics in position. (b) SEM picture of three hollow waveguides without the lid with widths of 90, 80, and 70 $\mu$m. The inset shows a detail of their low wall roughness.

The development of simple and robust biosensor devices that rely on the use of pure silicon-based hollow waveguides is described in this work. This structure exhibit some additional advantages such as improved chemical and mechanical stability, simpler fabrication technology requirements, potential low cost, and ease of surface modification for the immobilization of biological compounds. As a first approach, an enzymatic sensor based on the attachment of HRP to the inner walls of a hollow waveguide is described here. The waveguide core was filled with a transparent solution containing an appropriate enzyme substrate, which resulted in the generation of a colored product following the corresponding catalytic reaction. Such a reaction could thus be easily detected by absorbance measurements at an appropriate wavelength. With the use of this configuration, the sensing area corresponds to the whole waveguide core, so the sensitivity can be highly increased. Moreover, it is anticipated that the integration of such a sensor device within a simple microfluidic system is viable, because the hollow waveguides can also play the role of the microfluidic channels. To the best of our knowledge, this is the first absorbance biosensor based on pure silicon hollow waveguides presented to date.

## EXPERIMENTAL SECTION

**Fabrication of Hollow Waveguides.** In order to simplify the technology involved, the number of steps required to obtain the hollow waveguides were reduced. Deep reactive ion etching (DRIE)[14,15] was used to define a batch of 5 mm long channels with widths up to 80 $\mu$m on silicon. Thus, just one photolithographic step was needed to define the areas to be etched by the DRIE process.

**Hollow Waveguide Surface Modification.** In order to prepare the waveguide inner surface for biomolecule immobilization, two steps were carried out. First, the structures were dipped in a 10% HF solution during 10 s in order to ensure the thorough cleaning of the silicon surface. Second, an immersion of the waveguides in piranha solution (3:1 mixture of concentrated $H_2SO_4-H_2O_2$) for 10 min allowed for a light oxidation of the silicon surface. The waveguides were then thoroughly rinsed with DI water, dried under a $N_2$ stream, and stored in a sealed container for a few hours before use.

The waveguide surface silanization process was carried out in gas phase using a reaction chamber saturated with 3-(2,3-epoxypropoxy)propyltriethoxysilane (≥97%, Sigma-Aldrich Química S.A., Spain) overnight.[16] The resulting modified surfaces were rinsed with EtOH and dried under a $N_2$ stream. Then, they were incubated in a 1 mg/mL horseradish peroxidase (HRP, type VI, Sigma-Aldrich Química S.A) solution in 0.01 M phosphate buffer pH 7.5 (PB) for 1 h. In this process, HRP covalently binds to the epoxy-modified surface. Finally, the modified waveguides were rinsed in PB containing 0.02% Tween 20 (Sigma-Aldrich Química S.A.), followed by a thorough rinse in PB, in order to remove any noncovalently adsorbed HRP molecules from their surface.

**Optical Simulation and Characterization.** The optical behavior of the presented biosensor was simulated using the commercial software FIMMWAVE and FIMMPROP (Photondesign).[17] Simulated structures were carried out for a silicon hollow waveguide with a rectangular cross section of 80 $\mu$m × 50 $\mu$m and a length of 5 mm, having the waveguide core filled with the enzyme substrate solution.

In order to carry out these numerical analyses, the ABTS attenuation coefficient is required. The absorbance of substrate solutions containing 0.023 mg/mL HRP and increasing concentrations of $H_2O_2$ in the range of 10−1000 $\mu$M was measured at a set incubation time of 1 min, using a spectrophotometer (UV-2401PC, Shimadzu) in the visible region of the spectrum. PMMA cuvettes with a 1 cm path length were employed. From the recorded spectra, and considering the refractive index of 1.33 for the core and 3.82 for silicon, together with the silicon absorption coefficient fixed at 2800 $cm^{-1}$, the absorption coefficient of the waveguide liquid core at the working wavelength of 670 nm was estimated for the different $H_2O_2$ concentrations.

**Sensor Setup and Performance.** A 670 nm working wavelength luminescent diode (LED) was used as the optical source to characterize the fabricated biosensor. The LED was pigtailed to a 4 $\mu$m diameter single mode optical fiber. Light was injected into the waveguide by end-fire coupling and the output power collected using a 50 $\mu$m diameter multimode fiber connected to a silicon PIN photodiode. Figure 1a shows a schematic picture of the sensor setup with the input and output fiber optics held in

(14) Laermer, F.; Schilp, A.; Funk, A.; Offenberg, M. Presented at 12th IEEE International Micro Electro Mechanical Systems Conference (MEMS '99), Orlando, Florida, January 17−21, 1999.

(15) Bogaerts, W.; Baets, R.; Dumon, P.; Wiaus, V.; Beckx, S.; Taillaert, D.; Luyssaert, B.; Campenhout, J. V.; Bienstman, P.; Thourhout, D. V. *J. Lightwave Technol.* **2005**, *25*, 401−412.

(16) de la Rica, R.; Baldi, A.; Fernández-Sánchez, C. *Appl. Phys. Lett.* **2007**, *90*, 074102: 1−3.

(17) http://www.photond.com/. (Accessed 2007).

position. Alignment of the different components of the system was carried out with the aid of three *XYZ* micropositioners.

Sensor response to $H_2O_2$ was recorded using a 0.1 M acetate buffer solution pH 5 containing 50 $\mu$M 2,2′-azino-bis(3-ethylbenzthiazoline-6-sulfonic acid) (ABTS) and increasing concentrations of $H_2O_2$ in a range from 10 to 1000 $\mu$M. Both ABTS and $H_2O_2$ were purchased from Sigma-Aldrich Química S.A. A 4 $\mu$L drop of this solution was placed on the hollow waveguide input. The waveguide core volume (0.02 $\mu$L) was filled by capillary action. A time of 10 s was needed, after the hollow waveguide was filled with the liquid, in order to check that the input and output waveguide remain aligned to the biosensor. After that, the output light power was stable and it was then recorded for 10 min. The sensor response (output power transformed in absorbance units) recorded at 10 min incubation time was set as the analytical signal. Previous to the performance of a new measurement, the biosensor was dipped in PB for 10 min.

## RESULTS AND DISCUSSION

**Waveguide Fabrication Process.** To obtain an optimal confinement of the light in the hollow waveguides, verticality of the walls and the roughness on the inner surfaces are critical aspects. DRIE allowed vertical wall definition, showing angle values from the horizontal substrate of 89.1° ± 0.7°. The resulting average roughness values ($R_a$) on both the etched surface and walls were less than 5 nm and 57 ± 1 nm, respectively. Such values ensured an adequate light confinement in the fabricated structures.[18] Cross-sectional light confinement was attained by placing a polished silicon lid over the hollow core. This lid was fixed using a clamp. Figure 1b shows a scanning electron microscopy (SEM) picture of three hollow waveguides (without the lid). High quality walls with low roughness can be observed on the inset picture.

The simplicity of the fabrication process and the absence of multilayer structures or polishing steps make these structures ideal for the development of low-cost optical biosensors. The proposed silicon technology is CMOS-compatible, and therefore readout electronics, such as PIN photodiodes, could also be defined on the device, thus leading to a high degree of monolithic integration.

**HRP-Modified Silicon Surface.** Silanization of lightly oxidized silicon surfaces was easily carried out before fixing the silicon lid over the hollow core of the waveguides. Silanol groups generated at the surface of silicon readily react with the hydrolyzed methoxy groups of the functional silane molecule giving rise to stable siloxane bonds. Gas-phase silanization processes allowed for a more controlled modification of the surface and the avoidance of multilayer formation at the silicon surface. Silicon-modified surfaces bearing different chemically active groups can thus be achieved. The surface of the hollow waveguides was modified with an epoxysilane. HRP was further covalently bound to the silanized surface. Under the experimental conditions used for enzyme immobilization, covalent binding is more likely to take place by a nucleophilic attack of terminal amine groups of the protein to the epoxy ring giving rise to a $\beta$-hydroxy group and a stable secondary amine (see Figure 2). HRP stable anchorage to the silane surface was demonstrated by repetitive measurements using the same device. No loss of HRP activity was observed.

(18) Cadarso, V. J.; Llobera, A.; Salinas, I.; Izquierdo, D.; Garcés, I.; Domínguez, C. *Opt. Commun.* **2008**, *281*, 1568−1575.

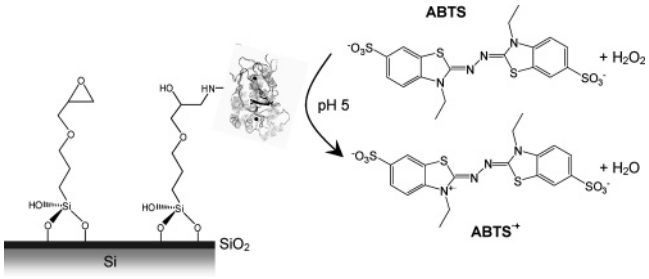


**Figure 2.** Scheme of the Si modification and subsequent HRP immobilization processes and corresponding enzyme reaction with colorless ABTS substrate to give green $ABTS^{\cdot+}$ cation radical product.

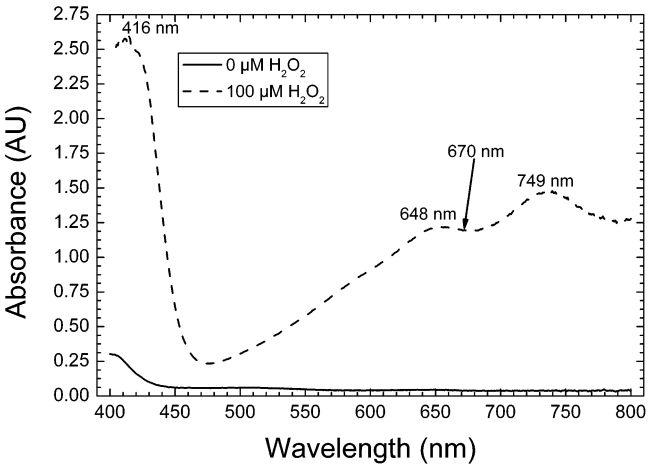


**Figure 3.** Absorbance spectra of HRP reaction medium containing 0 and 100 $\mu$M $H_2O_2$.

In case enzyme denaturalization occurred, complete removal of the attached enzyme molecules could be carried out by removing the lid and simply dipping the structure in 10% HF. Such treatment destroys the modified silane layer, thus obtaining a clean silicon surface. This process was carried out up to four times on the same structure in order to test the regeneration capacity of the presented waveguide structure.

**Sensor Response.** ABTS was chosen as the HRP cosubstrate to carry out the detection of $H_2O_2$. ABTS solutions, prepared as described above, are colorless. The corresponding catalytic reaction induces the oxidation of ABTS to give the $ABTS^{\cdot+}$ cation radical green-colored product (Figure 2). This was detected by absorbance measurements at 670 nm.

In order to estimate the attenuation coefficient of both the ABTS substrate and the $ABTS^{\cdot+}$ product, absorbance spectra were recorded in the visible region of the spectrum, in solutions containing 50 $\mu$m ABTS, 0.023 mg/mL HRP, and increasing concentrations of $H_2O_2$. Figure 3 depicts the spectra corresponding to $H_2O_2$ concentrations of 0 and 100 $\mu$M. On the one hand, it shows that the background signal corresponding to the absence of the target analyte in solution could be neglected. On the other hand, the presence of the analyte in solution gives rise to three distinguishable peaks at 416, 648, and 749 nm wavelengths. An absorbance value of 1.25 AU was measured at the working wavelength of 670 nm.

The total losses of the biosensor approach in the absence of $H_2O_2$ were 3.7 dB. The response of the hollow waveguide biosensor approach to $H_2O_2$ was linear in a concentration range from 10 to 300 $\mu$M. The corresponding calibration curve is

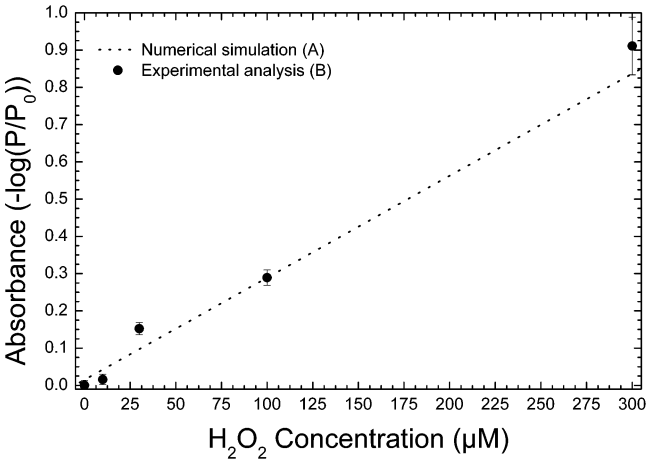


**Figure 4.** Graph of numerically simulated (A) and empiric (B) sensor response. The sensor was fabricated using a hollow waveguide of dimensions 50 $\mu$m $\times$ 80 $\mu$m $\times$ 5 mm (height/width/length).

depicted in Figure 4, together with the results obtained from the simulation studies. These calibration experiments were repeated up to four times using the same hollow waveguide transducer by performing a surface regeneration, as described in the Experimental Section. Both empiric and simulated results are in excellent agreement. A sensitivity of $(3.0 \pm 0.1) \times 10^{-3}$ AU/$\mu$M, a limit of detection (LOD) of $20 \pm 1$ $\mu$M (in accordance to the $3\sigma$ IUPAC definition), and a signal-to-noise ratio (SNR) around 20 dB for the buffer solution was achieved by experimental measurement. Simulation studies predicted a biosensor sensitivity of $2.7 \times 10^{-3}$ AU/$\mu$M, a LOD of 5 $\mu$M, and a linear response in the same concentration range of 10−300 $\mu$M $H_2O_2$.

The sensor response to $H_2O_2$ follows Michaelis−Menten kinetics in a concentration range up to 1000 $\mu$M. With the use of Lineweaver−Burk linearization, the apparent Michaelis−Menten constant ($K_M^{app}$) was estimated to be 0.44 mM. From the absorbance spectra recorded with HRP in solution, $K_M^{app}$ of the enzyme in solution was estimated to be 0.68 mM, under the same experimental conditions. These values indicate the higher affinity of the immobilized enzyme toward the $H_2O_2$ substrate and provide evidence to support the suitability of the immobilization protocol on the walls of the hollow waveguide structure.

## CONCLUSION

With the use of HRP as a model bioreceptor, a biosensor approach based on a pure silicon hollow waveguide structure for the detection of $H_2O_2$ was developed. Colorless ABTS enzyme cosubstrate undergoes a catalytic oxidation to give the green-colored radical cation $ABTS^{\cdot+}$. Hence, an absorbance detection mode at a 670 nm wavelength was applied. An empiric characterization and numerical simulation of the sensor response was carried out. The calibration parameters obtained in both cases showed excellent agreement. The ease of fabrication of the reported hollow waveguide transducers together with the straightforward modification of their inner walls with a bioreceptor may result in the development of low-cost, easy-to-use biosensor platforms. Besides, taking into account that the waveguide fabrication process is CMOS compatible, it is anticipated that such platforms could be easily integrated in microfluidic systems also including all the electronic circuitry, which will enable the easy development of lab-on-a-chip devices.

## ACKNOWLEDGMENT

This work has been made possible with funds of the Project P. Cezanne, IST-2005-2.5.2-031867 funded by the E.U. V. J. Cadarso acknowledges the Consejo Superior de Investigaciones Científicas (CSIC) for the award of a studentship of the I3P program, cofinanced by the European Social Fundation. C. Fernández-Sánchez and A. Llobera thank the Spanish Ministry of Science of Education for the award of a Ramón y Cajal contract. M. Darder acknowledges the CSIC for an I3P postdoctoral contract.

Received for review November 6, 2007. Accepted January 23, 2008.

AC702293R